

# Automatic detection of circular depressions in digital elevation data in the search for potential Norwegian impact structures

Svein Olav Krøgli, Henning Dypvik & Bernd Etzelmüller

Krøgli, S.O., Dypvik, H. & Etzelmüller, B.: Automatic detection of circular depressions in digital elevation data in the search for potential Norwegian impact structures. *Norwegian Journal of Geology*, Vol. 87, pp. 157-166. Trondheim 2007. ISSN 029-196X.

Presently, 174 impact craters are proven on Earth, and of these 10 are located in Finland, 6 in Sweden and only 2 in Norway (Gardnos and Mjølner). A pattern matching algorithm (correlation) based on 100 m digital elevation data was used in a regional study to discover circular depressions in the search for possible new Norwegian impact structures. By applying this technique to detect depressions of 5 – 10 km diameter in Finnmark, northern Norway, about 23 large circular structures were found in a 14,000 km<sup>2</sup> area of Precambrian rocks. Circular features are clearly displayed in the detected structures. The large number of candidates in this area, however, makes field inspection inconvenient and time consuming, and supplementary screening methods should be considered to help reduce the number.

Krøgli, S.O., Dypvik, H., Etzelmüller, B., Department of Geosciences, University of Oslo, P.O. Box 1047 Blindern, No - 0316 Oslo, Norway. E-mail: s.o.krogli@geo.uio.no, henning.dypvik@geo.uio.no, bernd.etzelmuller@geo.uio.no

## Introduction

Impact structures are formed by collisions of comets and asteroids with planets or moons, and these crater structures may be preserved for millions of years. The general understanding of impact cratering and its significance for the Earth's development has increased dramatically during last decades. This is a result of intensive exploration of our solar system and the geological structure of planets. Planetary surface analysis shows that most of the planets have geomorphologies strongly influenced by impact cratering (Lowman 1997). Today we know that impact processes and crater formation have been (and will be) important processes for the development of our solar system (Melosh 1989; Montanari & Koeberl 2000).

On Earth 174 impact structures have been found so far (Earth Impact Database 2006). These craters seem unevenly distributed, partly the result of observations being focused on populated areas, rather than on less accessible locations. In Fennoscandia eighteen proven structures (Earth Impact Database 2006) have been found; ten in Finland, six in Sweden and only two in Norway (Gardnos and Mjølner) (Fig. 1). The number of suggested ones is much higher (Abels et al. 2002), and in Norway we have a new, very promising candidate in the Ritland structure (Rogaland) (Fig. 1). Due to the varied surface geology and its areal extent it is difficult to calculate the expected number of impact structures of 5 – 10 km diameter in Norway. In this experiment we have searched for 5 – 10 km diameter structures in a 14,000 km<sup>2</sup> area of Precambrian rocks in Finnmark (Fig. 2).

When attempting to detect impact craters a simple but appropriate question might be: What do impact craters look like, and are such structures present in Norway? Normally the crater itself and its circular shape are regarded as important arguments for impact identification, in addition to structural and mineral evidence (Montanari & Koeberl 2000). The first possible registration of a crater is therefore often related to the identification of a circular surface structure. As the proven structures have large diameters (0,015 - 300 km (Earth Impact Database 2006)) and are dispersed over large areas, aerial photos, optical- and radar satellite images (e.g. Araujo et al. 2001; Chicarro et al. 2003; Earl et al. 2005) and coarse digital elevation models (DEM) (e.g. Portugal et al. 2004) have been commonly used in screening surveys.

There are mainly two important families used in pattern recognition of impact structures (Di Stadio et al. 2002); a) voted methods like the circular Hough Transform (e.g. Matsumoto et al. 2005; Portugal et al. 2004) and b) matching methods (e.g. Magee et al. 2003). In the approach presented below we used a digital matching technique, known from image analysis (e.g. Efford 2000; Gonzalez & Woods 1993) and automatic photogrammetric elevation generation (e.g. Heipke 1997; Schenk 1999).

The objective of this study was to develop an automatic technique to identify potential impact structures on the basis of morphometric analyses of a continuous topographic surface. Based on elevation data the aim was to find impact structure candidates, with a geometric shape matching the shape of a typical terrestrial impact

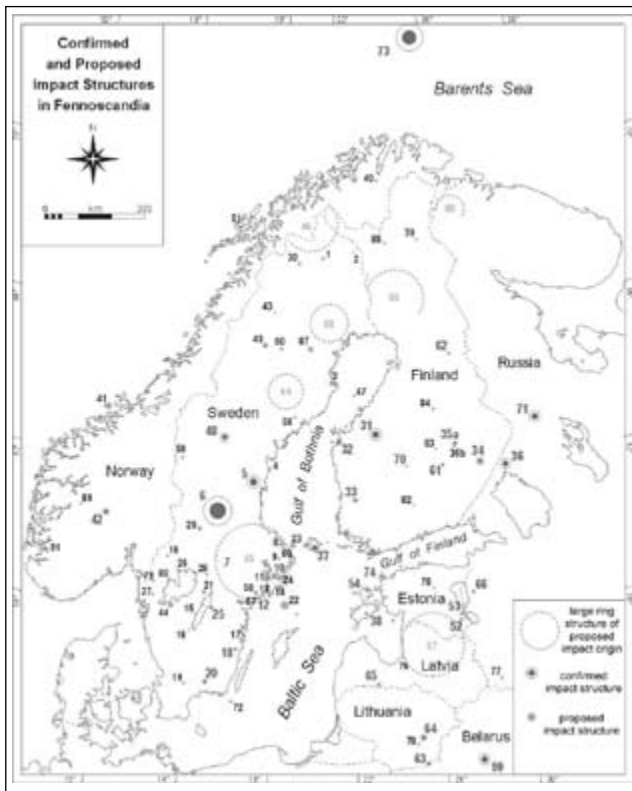


Fig. 1. The distribution of confirmed and proposed impact structures in Fennoscandia (Norway: 42 Gardnos, 73 Mjølneir, 91 Ritland). The figure is modified from Abels (2006).

crater of 5 – 10 km diameter. Analyses of the formation mechanics of the candidates must be evaluated by subsequent field inspections and laboratory analysis.

## Geological setting

Norway comprises the western part of the Scandinavian Peninsula. The bedrock geology of Norway is dominated by Precambrian basement rocks (e.g. granites, gneisses, amphibolites and meta-sediments) and Caledonian successions (mostly Precambrian rocks and metamorphic Cambro-Silurian sediments stacked in nappe units). Limited areas of Devonian to Permian sediments and volcanics are also present (Fig. 2). The larger part of the bedrock is, however, covered by various Quaternary formations of mainly marine, glacial and fluvial origin. Geomorphologically the present topography of Norway is governed by peneplanation and stripping of marine strata during the Mesozoic (Lidmar-Bergstrøm et al. 2000; Peulvast 1985), a Tertiary uplift (Gjessing 1967; Strøm 1948) and related fluvial-dominated landscape formation in a warmer and partly drier climate than today (Gjessing 1967; Lidmar-Bergstrøm et al. 2000; Strøm 1948), followed by numerous Quaternary glaciations (Kleman & Borgstrøm 1994). The latter accentuated the Tertiary fluvial valley pattern, while areas in central and northerly mountainous areas underwent little or

no erosion due to the thermal conditions of the ice sheets (Lidmar-Bergstrøm et al. 2000, Sollid & Sørbel 1994).

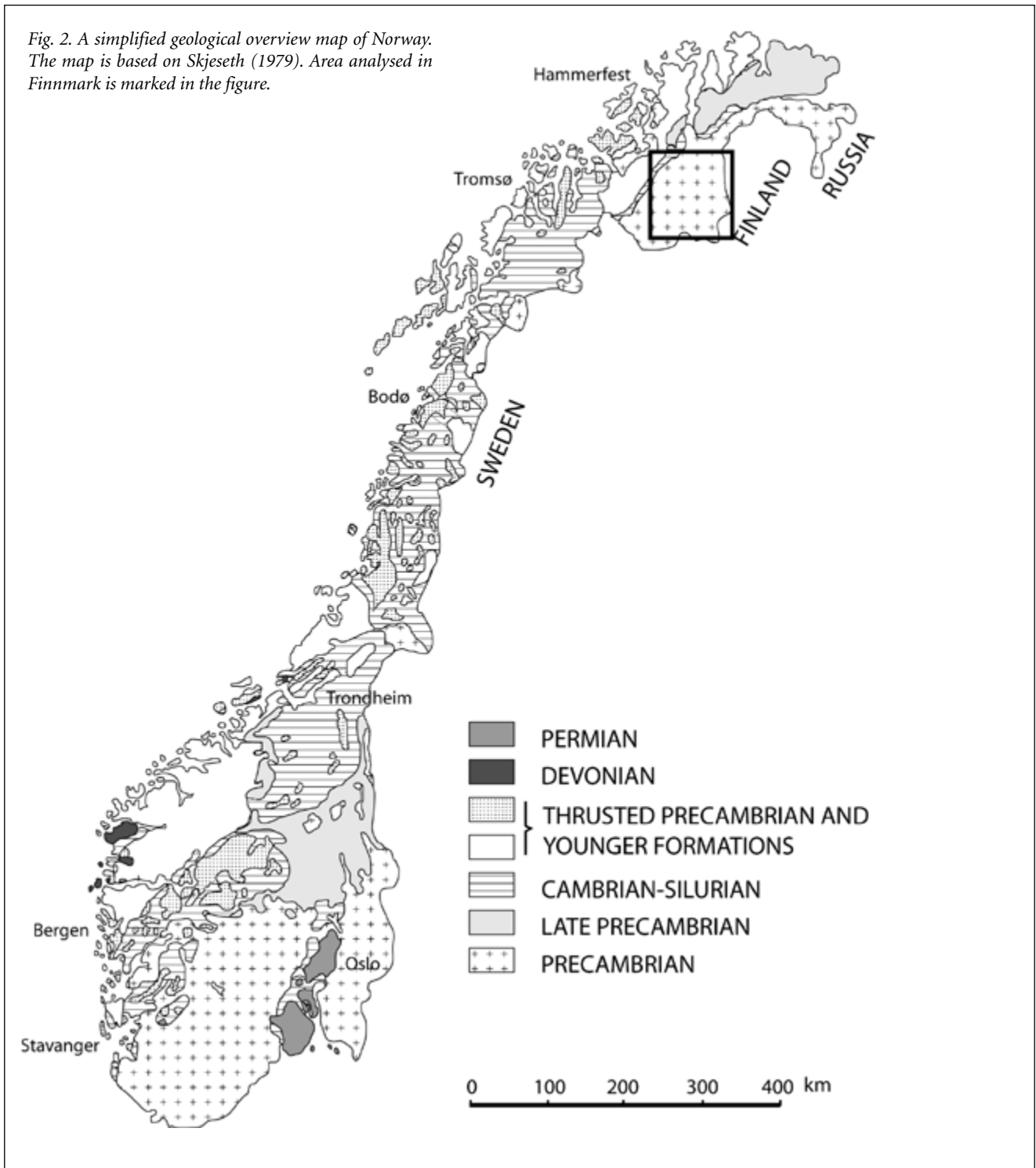
Impact structures can be expected in all kinds of terrain, but with varying preservation potential. The oldest rocks, e.g. Precambrian gneisses and meta-sediments, are normally the hardest and may therefore have a good chance of displaying impact structures, due both to high age and competence. In contrast, the younger Cambro-Silurian formations, less consolidated sedimentary rocks and loose sediments will, as target rocks, not preserve impact structures as well. The Caledonian orogeny may also have altered possible earlier structures. The last glaciations in Scandinavia both eroded and covered (by sedimentation) possible pre-Quaternary impact structures. Based on this information, Finnmark appears as a suitable test area for further impact studies (Fig. 2).

## Impact crater morphology

When celestial bodies (asteroids and comets) collide with planets or moons, the shape of the resulting crater is dependent on target material and the size, velocity and angle of the impacting body. The shapes and sizes of impact structures change with crater diameter, and fresh-appearing impact structures on the Moon illustrate this size-morphology relationship (Melosh 1989). The smallest impact craters have a simple bowl-shaped appearance, and as crater diameter increases, rim terracing and central peaks are more common. Crater morphology displays the same progression throughout the solar system, including the Earth, but the less well preserved terrestrial impact structures make them more challenging to classify (Earth Impact Database 2006). On Earth, the three basic types of impact structure are 1) simple structures, with a raised rim surrounding a bowl-shaped depression, 2) complex structures, larger in diameter, with a central peak, surrounded by an annular trough and a slumped rim (e.g. Grieve 1990; Melosh 1989) and 3) the even larger and more rare peak ring craters, consisting of a central peak (possibly with a depression) and possibly several ring structures creating annular basins (e.g. Turtle et al. 2005). The transition between simple and complex craters occur at diameters of about 2 km or 4 km, in sedimentary or crystalline rocks respectively (Grieve 1990).

Global processes acting on the surface of the Earth will eventually leave more poorly preserved impact structures (Turtle et al. 2005), which can be hard to distinguish from their surroundings. Their appearance then reflects geologic activity and post-impact physical processes (e.g. erosion, subduction). Fresh looking craters (e.g. Barringer crater, Arizona, USA) are easily recognized, but older impact structures may be eroded and filled with sediments. High velocity impacts produce circular craters, even at angles of low incidence (Melosh 1989). The presence of a circular-shaped depression is characteristic for

Fig. 2. A simplified geological overview map of Norway. The map is based on Skjeseth (1979). Area analysed in Finnmark is marked in the figure.



fresh impact structures and provides important information for use in the following analyses.

The geologically active Earth causes terrestrial impact structures to exhibit a high degree of variation as regards morphological characteristics and few fresh examples are left (Earl et al. 2005; Turtle et al. 2005). Still, some size characteristics are needed in order to construct a proper template. When searching for impact structures between 5 and 10 km in diameter, size-morphology relations for plausible impact structure depths, as presented in

Grieve & Pesonen (1992), were used in the analysis. They divide the final morphology of complex terrestrial craters according to whether the target rocks are sedimentary or crystalline. This is due to the strength differences between the two. Complex craters are shallower when formed in sedimentary target material than in crystalline target material. In this analysis the equation (1) for sedimentary targets is used (Grieve & Pesonen 1992).

$$d_a = 0.12D^{0.30} \tag{1}$$

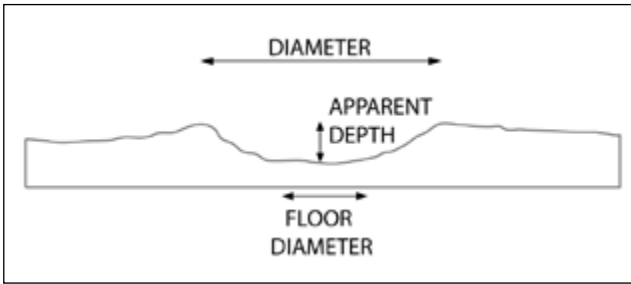


Fig. 3. Characteristic crater dimensions (diameter, apparent depth and floor diameter) displayed on a topographic profile. Modified from Pike (1977).

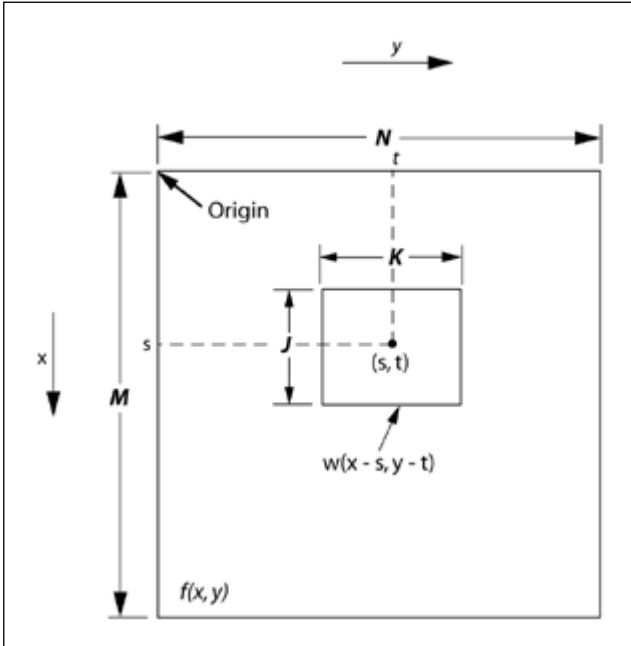


Fig. 4. Image and template arrangement for obtaining the correlation of respectively  $f(x,y)$  of size  $M \times N$  and  $w(x,y)$  of size  $J \times K$  at points  $(s,t)$ , according to equation (3). The origin of  $f(x,y)$  is at its top left and the origin of  $w(x,y)$  at its centre. For any value of  $(s,t)$  inside  $f(x,y)$ , the application will yield one correlation value. As  $s$  and  $t$  vary,  $w(x,y)$  moves around the image area (Gonzalez & Woods 1993).

where  $d_a$  is apparent depth (km), and  $D$  is diameter (km) (Fig. 3). The sedimentary target rock equation is chosen because this gives a shallower depth than the crystalline equation and may fit better the possibly new Norwegian impact structures after years of erosion.

A relation between crater diameter and floor diameter (2) based on lunar statistics (Pike 1977) is used to determine the size of a flat crater floor in the model.

$$D_f = 0.031D_r^{1.765} \quad (2)$$

where  $D_f$  is the crater floor diameter, and  $D_r$  is the rim-crest diameter. It does not apply to craters less than 5 km in diameter (Pike 1977). The use of a rim-crest diameter in this equation and a probably apparent diameter in equation (1), implies that the crater floor diameter may be a bit undersized.

## Data and methods

### Digital elevation data

This study is based on digital elevation data in the computer represented as regular square grid models or arrays of elevation values. Such digital representation of the topographic surface is static and scale dependent since the size of the cells (pixels) building the terrain model is unchangeable (Burrough & McDonnell 1998). The matrix structure will allow programming of relatively complex algorithms, which can be easily used for digital elevation model (DEM) manipulation. Thus, this type of grid structure provides good possibilities for modelling any type of surface, and to investigate spatial interactions of features, being close or remote from the processed location (DeMers 2002). The resolution (scale) of the grid data is the relation between pixel size and size of the cell on the ground (Burrough & McDonnell 1998). When using grid-based DEMs to recognize landforms it is important to consider the resolution relative to the landform size (DeMers 2002). For the search of impact structures of 5 – 10 km diameter, we found a 100 m resolution satisfactory for these first analyses. A 3 x 3 kernel neighbourhood mean filter was applied to the elevation data to reduce noise.

### Matching by local correlation

Template matching is a technique to measure the similarity between an unknown image and a known image acting as a feature model or template (Gonzalez & Woods 1993). Correlation analysis was used to describe the similarity between the known image (template)  $w(x,y)$  of size  $J \times K$  within an image  $f(x,y)$  of size  $M \times N$ , where it is assumed that  $J \leq M$  and  $K \leq N$  (Fig. 4). The result of each correlation analysis is an image, the size of image  $f(x,y)$ , where each pixel consists of a correlation value. The calculations are performed in the image region where  $w$  and  $f$  overlap, and high values of correlation indicate a match between  $w(x,y)$  and  $f(x,y)$  (Gonzalez & Woods 1993). Near the edges of image  $f$ , there will be no full overlap with  $w$ , and hence along the borders of the image  $f(x,y)$  there will be an area, half the size of  $w$ , where no correlation calculations are performed.

In our study we used spatial domain methods, where the procedures operate directly on the pixel values, while frequency domain methods operate on the results of a Fourier transform. The algorithm presented is based on a spatial domain matching procedure for calculating correlation coefficients (Gonzalez & Woods 1993), equation (3):

$$\gamma(s,t) = \frac{\sum_x \sum_y [f(x,y) - \bar{f}(x,y)][w(x-s,y-t) - \bar{w}]}{\left\{ \sum_x \sum_y [f(x,y) - \bar{f}(x,y)]^2 \sum_x \sum_y [w(x-s,y-t) - \bar{w}]^2 \right\}^{1/2}} \quad (3)$$

where  $s = 0, 1, 2, \dots, M - 1$ ,  $t = 0, 1, 2, \dots, N - 1$ ,  $\bar{w}$  is the average value of the pixels in  $w(x,y)$  (computed only

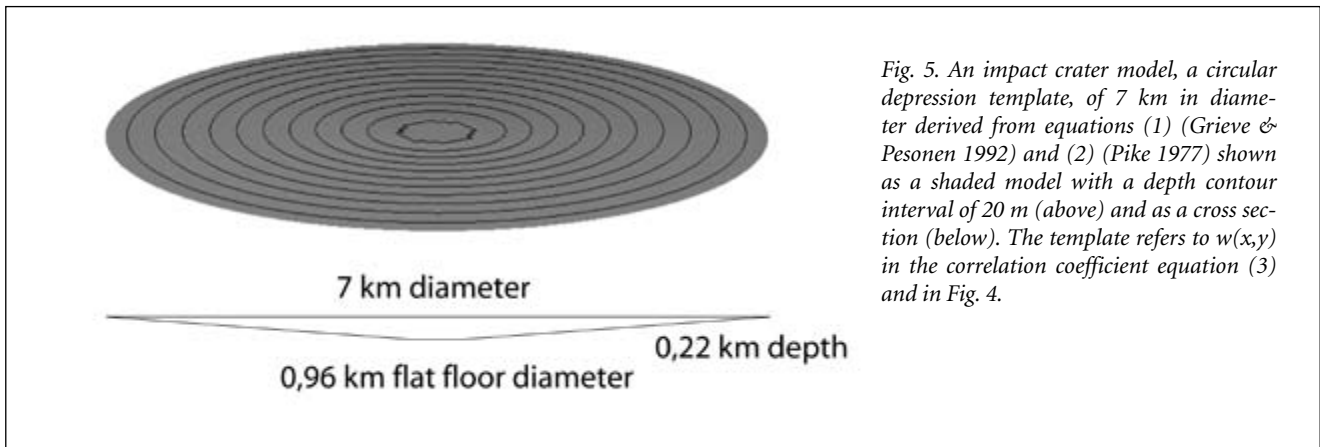


Fig. 5. An impact crater model, a circular depression template, of 7 km in diameter derived from equations (1) (Grieve & Pesonen 1992) and (2) (Pike 1977) shown as a shaded model with a depth contour interval of 20 m (above) and as a cross section (below). The template refers to  $w(x,y)$  in the correlation coefficient equation (3) and in Fig. 4.

once),  $\bar{f}(x,y)$  is the average value of  $f(x,y)$  in the region coincident with the current location of  $w$ , and the summations are taken over the image coordinates (pixels) common to both  $f$  and  $w$ . The correlation coefficient  $y(s,t)$  is scaled (normalised with respect to both image and template) in the range -1 to 1, independent of scale changes in the amplitude of  $f(x,y)$  and  $w(x,y)$  (Gonzalez & Woods 1993). Correlation analysis works well only if the size and orientation of the feature of interest are known and this information is used to design an appropriate template. If the size and orientation of the feature varies, a range of templates needs to be generated and each of them correlated with the image (Efford 2000). The automatic detection algorithm calculates the correlation between two datasets with a grid structure. It is a combination of C++ code and Arc Macro Language (AML). Input to the algorithm are an elevation data grid,  $f(x,y)$ , where the search for impact structures will take place, and a template grid,  $w(x,y)$ , smaller in size and representing the circular depressions to be found. Output of the algorithm is a map consisting of a similarity value (correlation coefficient) between the image and the template for every pixel position  $y(s,t)$  (Fig. 4).

#### Impact structure templates

In the correlation analysis performed, the unknown image represents the topography of the study area, in this case a part of Norway and consists of a DEM, while the template is a smaller DEM representing a theoretically defined impact crater. The general crater morphology forms the basis for creating this crater-shaped template (model). By using equations (1) and (2) to create templates and then including a degree of variation in the analysis, a match with terrestrial formations should be possible. Six templates of diameters 5 km, 6 km, 7 km, 8 km, 9 km and 10 km were made, based on these equations. They have a circular shape and the crater rim-walls were given a linear outline due to their most likely appearance after years of erosion. The crater floor is stipulated flat (Fig. 5). These models were used as templates in the regional analysis (template matching). They have the same resolution as the image, and

the pixel values are of the same type and range as the pixels in the image.

#### Test area

The algorithm was tested on a synthetic 2,000 km<sup>2</sup> flat area, including one depression and one peak. The depression and the peak represent opposite, but similar geometries as the 5 km diameter template. By running a correlation analysis with a 5 km template and the test area, the correlation matching pattern of the template with “itself” is displayed. The correlation values show that in an ideal situation with a complete match, the pattern makes a circular formation with a correlation high of 1 and a negative correlation high of -1 (Fig. 6). A positive correlation as high as possible is preferred in the analysis, but also a value that picks out some candidates. The correlation coefficients tend, in a larger area, to be approximately normally distributed. A global threshold based on Niblack's (1986) method is set to  $t = \mu + w \cdot c$ , where  $\mu$  is the mean value,  $\sigma$  is the standard deviation of the correlation coefficient values, and  $w$  is an input weight. The threshold will divide the coefficient values into two classes, interesting (high values) and not interesting (low values). To keep the most promising candidates in each diameter size class, the same rule (a value of  $w$ ) applies to all (5 – 10 km) correlation value images. It will still be a low correlation coefficient (ca. 0.50 – 0.65 for  $w = 2 - 2.5$ ) compared to more ideal statistical solutions. This is a necessity because of the high variability of the circular depressions to be detected.

Pixel values above the threshold and within the immediate eight-cell neighbourhood of other pixels with higher values than the threshold, were spatially connected into a region. Area and perimeter were calculated for each region. The attribute roundness for a region can be described by  $4\pi \cdot \text{area} / \text{perimeter}^2$ , where the value for a circular disk is 1, otherwise less than 1. Identified candidates were regions having a roundness value above the algorithm input-roundness parameter.

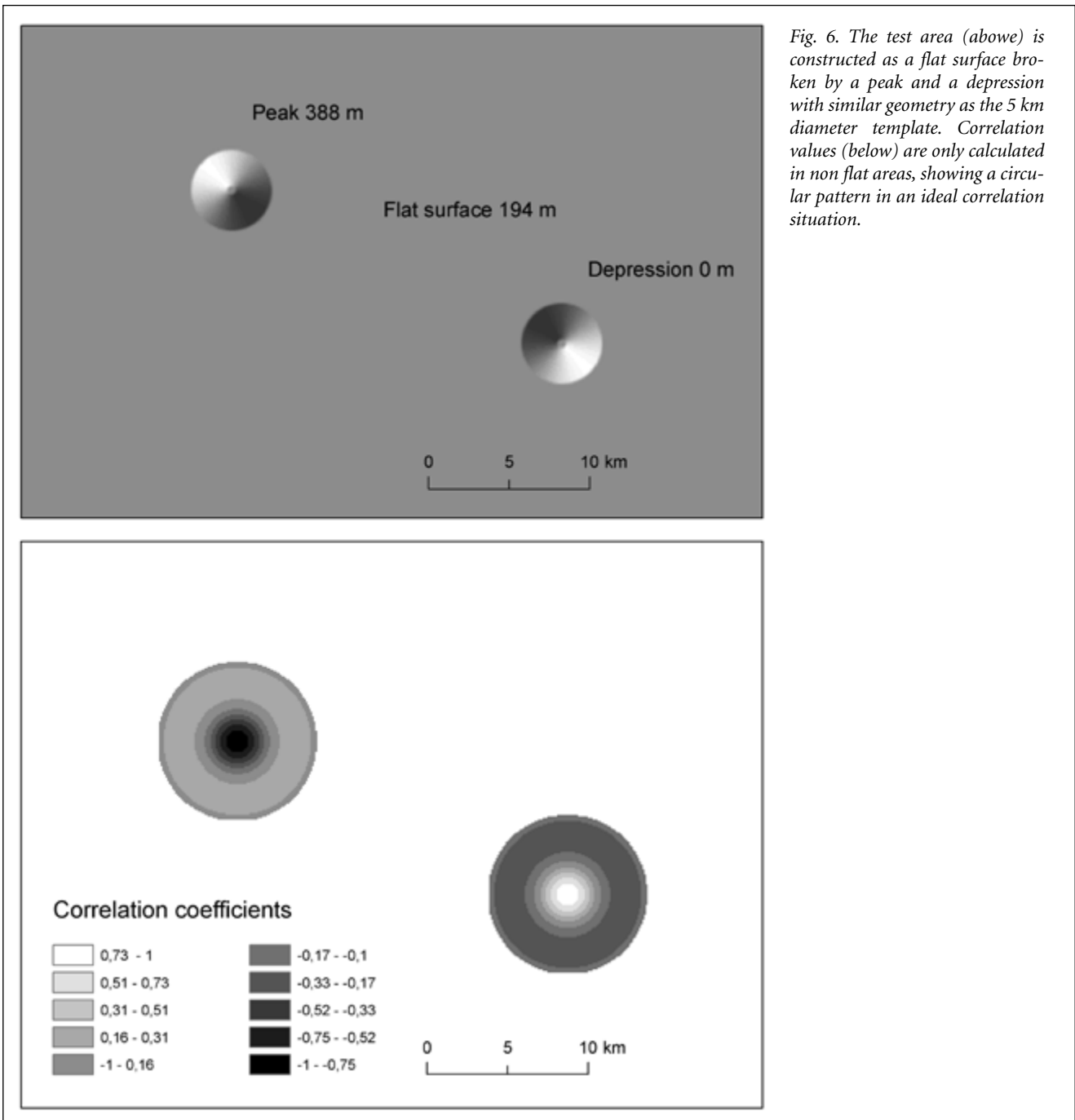


Fig. 6. The test area (above) is constructed as a flat surface broken by a peak and a depression with similar geometry as the 5 km diameter template. Correlation values (below) are only calculated in non flat areas, showing a circular pattern in an ideal correlation situation.

## Results

Figure 7 displays the various steps using the 8 km template, parameters  $w = 2.3$  and  $roundness = 0.5$ . These parameters and the range of templates (5 – 10 km) were applied on an area 14,000 km<sup>2</sup> in the county of Finnmark, northern Norway (Fig. 2), an area of mostly Precambrian basement rocks. The analysis yielded 23 circular depressions when not counting overlaps between the templates (Fig. 8). This procedure detects areas with different grades of circular shapes. When studying the detected structures in more detail, they also show hits of circular features in other close diameter intervals, although the template was set to specific diameter values. In such cases the template may hit and correlate with a curved feature (wall)

which is part of a smaller or larger structure.

102 structures were detected in a primary analysis of digital elevation data covering Norway with the 5 km diameter template,  $w = 2.5$  (threshold then becomes 65.98) and  $roundness = 0.5$ . This number is too large for realistic field investigations, but during the screening studies we still want to keep a relative high number of structures for further analysis. The Gardnos impact structure, now seen as a circumform hanging valley, is located between the villages Gol and Nesbyen. In the regional analysis it gave the following maximum correlation coefficient values inside its boundaries: 0.52 (5 km), 0.47 (6 km), 0.41 (7 km), 0.35 (8 km), 0.37 (9 km) and 0.41 (10 km). Even if it turns up with a relative high cor-

relation coefficient in the 5 km case, this is partly due to coincidences of later landscape formation, which may to some extent reflect the impact event.

## Discussion

The geometrical analyses display several circular features, partially matching the pre-described structure, and thereby sites of potential impact structures. Of these, at the best, only very few might have impact origin, when compared to the size distribution in Finland (4 impact structures in the interval 5 – 10 km) and Sweden (2 impact structures in the interval 5 – 10 km). The high number of potential Norwegian structures (102 of approximately 5 km diameter for Norway and 23 of 5 – 10 km diameter for a 14,000 km<sup>2</sup> area in Finnmark) and consequently a large number of false candidates are not suitable for a time saving search method. There are ways to restrict or vary the method:

- 1) The crater template appearance can be based on other equations or models, and thereby give different representations of impact structures (e.g. a template with non-linear walls).
- 2) The correlation coefficient threshold is the factor that determines how similar to the template the potential areas would appear, and a higher threshold (weight) would leave less circular depressions. A higher roundness value will leave fewer candidates.
- 3) The DEM and template spatial resolution will affect the results, and other resolutions may lead to different discoveries. But it is not necessarily true that a DEM with a finer resolution will give an increased spatial accuracy in terms of landform identification, since a finer-grained DEM may be more sensitive for other types of errors (DeMers 2002).

The Hough transform was developed to identify lines in images (Hough 1962). This technique, modified to identify circles or ellipses, and by applying different pre- and post-processing procedures, has shown promising results in detecting circular shapes in satellite images and DEMs of planetary bodies (e.g. Bruzzone et al. 2004; Earl et al. 2005; Kim et al. 2004; Matsumoto et al. 2005). In the presented template matching of this paper, the use of DEMs as input gives us an opportunity to take advantage of the horizontal profile (e.g. a depression) in addition to the vertical profile (circular shape). The variability of terrestrial impact structures in relation to topography requires a method that can handle this. The possibilities of the presented method to vary the threshold, the roundness value and vary the templates (e.g. topographic depression, linear or curved walls, flat or open crater floor), make template matching a convenient choice of technique.

A drawback is the computational time. The analysis performed with template diameters of 5 – 10 km in the

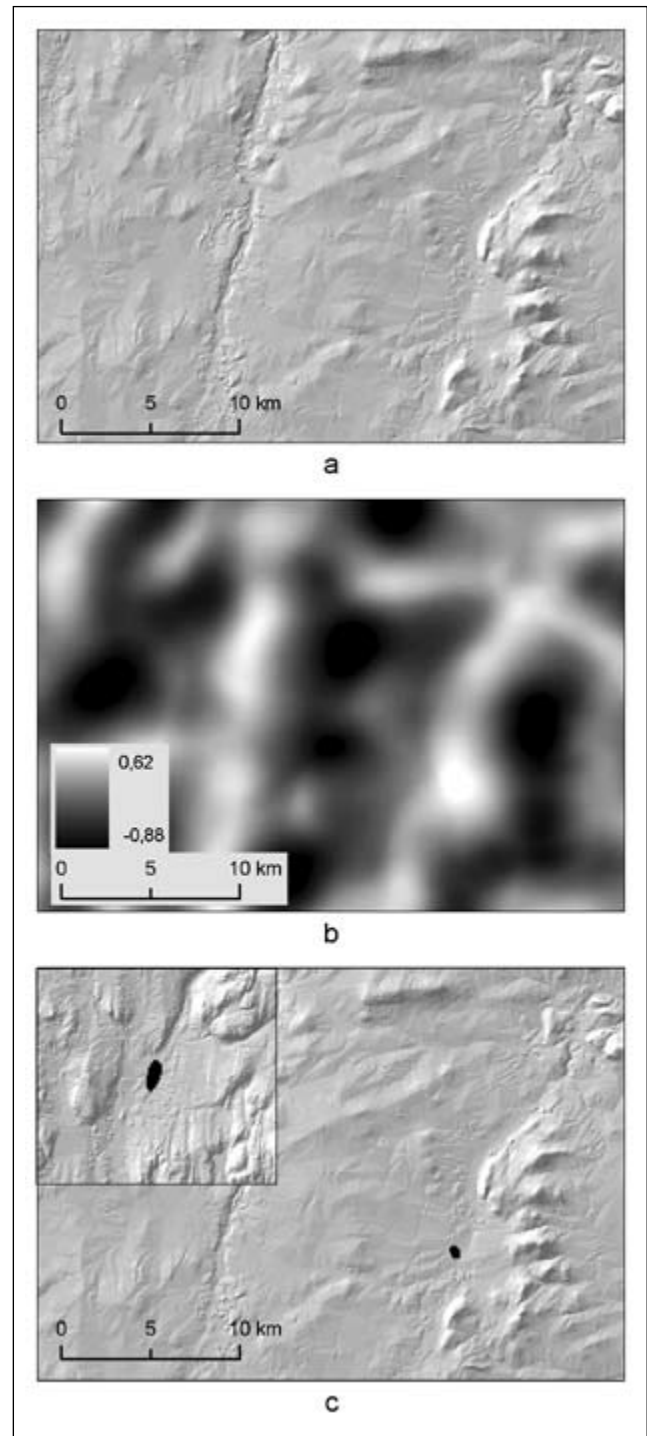


Fig. 7. Part of the area covered in Fig. 8, showing the steps of the algorithm: A shaded elevation model of the elevation data (a), a map of correlation values as computed by the algorithm for the 8 km diameter template (b). The correlation coefficients have values between -0.88 and 0.62, marked by dark to bright pixels. These values are divided into two classes by a threshold of 0.59 ( $w = 2.3$ ), where black coloured pixels have higher values than the threshold and pixels of lower values than the threshold are not displayed (c). The black coloured pixels are then grouped. In this small area the result is one group (c). A roundness value is then calculated for the group which is kept, because it has a roundness value above the input parameter (roundness = 0.5). An inserted map in the upper left corner (c) displays a group, at the same scale but from a different location, with a roundness value below the input parameter and subsequently will be removed.

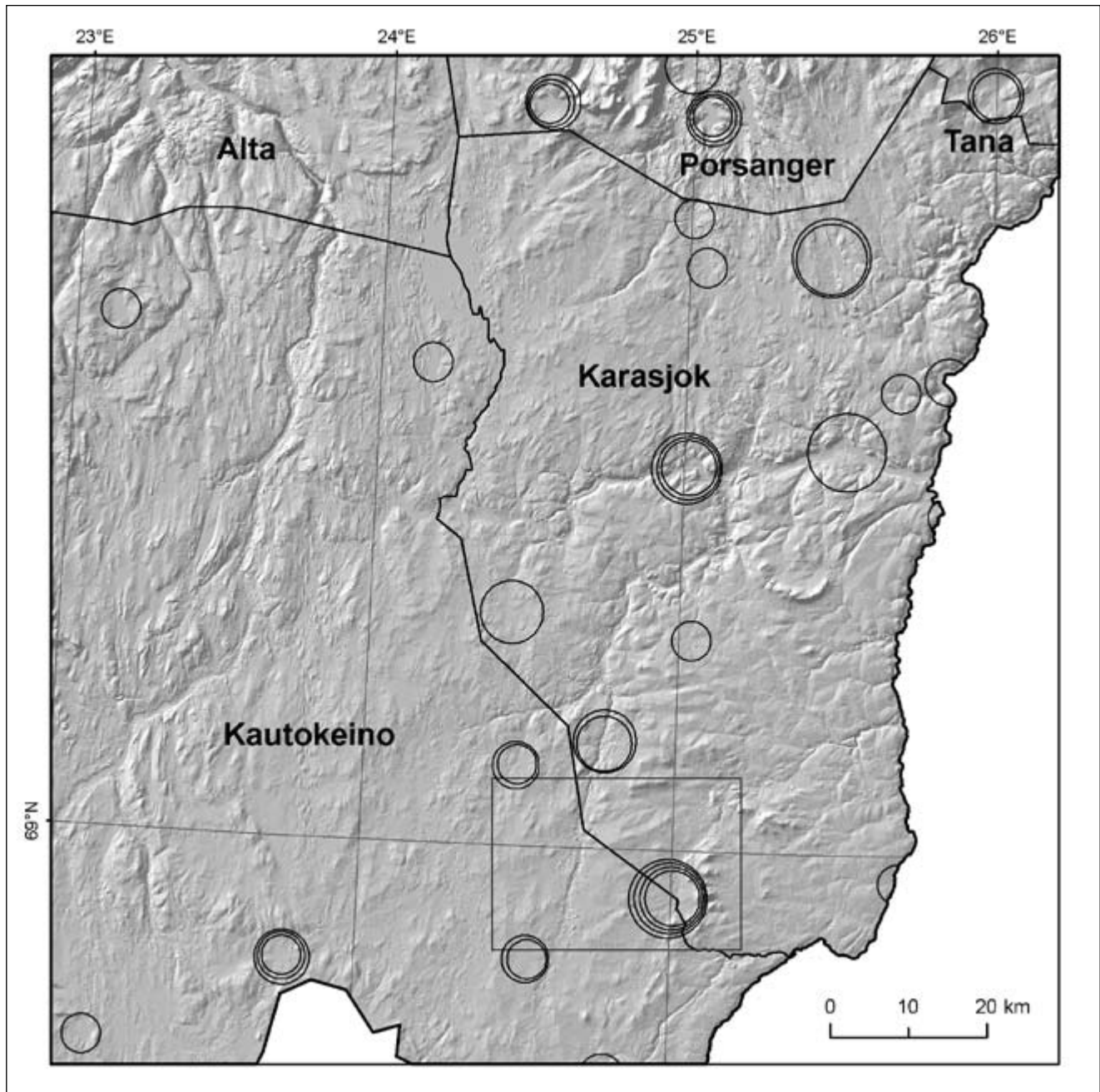


Fig. 8. An area of Finnmarksvidda including the municipality Karasjok and parts of Kautokeino, Alta, Porsanger and Tana, displaying detected circular depressions. For regional location see Fig. 2. The circular depressions are shown with circular symbols of diameters 5 – 10 km, the diameter referring to the template diameter detecting the individual structure. It shows 23 depressions, not counting overlaps between templates. The position of Fig. 7 is shown by the inserted square. Map projection: UTM EUREF89/WGS84 zone 35.

Finnmark area took several hours, and with larger templates it would take even longer. There is a possibility to compute the correlation in the frequency domain, using a fast Fourier transform algorithm to obtain the forward and inverse transforms. This is often a more effective solution (Gonzalez & Woods 1993). The spatial domain method used here is still a preferred option because of the convenient grid structure of the elevation data, and thereby an easier result interpretation.

The correlation function was normalized for amplitude

changes via the correlation coefficient and for orientation via its circular symmetry, but it can be difficult to obtain normalization for changes in size. Such changes involve spatial scaling, a process that requires a high amount of computation (Gonzalez & Woods 1993). In the presented analysis such normalization was not performed, but six different-sized templates were used to inspect the range of potential structures in the 5 – 10 km interval. An inspection of the results showed that the method gave hits of circular features of diameter values close to the template diameters as well. In this way the intervals between the templates may be covered.



The diameter/depth and diameter/crater floor diameter relations of equations (1) and (2) were used to create the applied templates. It is a huge simplification to describe the shape of impact structures with just these two size morphology equations. In addition to the active surface processes working on the Earth and changing the crater appearance, the initial crater size depends on the target's surface gravity conditions (e.g. Lowman 1997). The crater floor equation is based on statistics from the Moon and a transfer of the relationship to the Earth may introduce some error. However, application of a too specified crater morphology can be misleading, since similarly sized terrestrial impact craters often exhibit contrasting characteristics (Earl et al. 2005). It is the template simplification and a correlation threshold set to less than the maximum result correlation coefficient value that makes it possible to pick out areas in the landscape, but finally resulting in a large number of circular depressions.

A high match percentage means that the structure has approximately the same shape as the circular template, but it could have been formed in several ways. Equation (1) is based on data from only five craters (Grieve & Pesonen 1992) and equation (2) is based on lunar statistics. This rather confined foundation, and the high degree of variation of known impact structures, contributes to the analytical uncertainty. The large number of candidates might call for a manual inspection of the digital data before field investigations, for example to exclude the less promising sites based on non crater-like features. Another solution could be to filter the results with other data or additional analysis. This could involve comparing the theoretical circular sites with geological or geophysical information, a possible part of the automatic detection. An improved exercise would need to compute different time models reflecting the various environmental settings through geological time, presently an immense task. Therefore the next step to evaluate the formation mechanisms of the detected depressions would be field inspections of the various structures.

## Conclusions and further studies

From this study the following conclusions can be drawn:

- a) An automatic correlation algorithm based on gridded DEMs on a regional scale seems suitable to identify depressions with circular features. This is a first approach and represents an oversimplification regarding automatic impact crater search.
- b) These morphometrical DEM analyses provide a powerful and inexpensive tool for first landform assessments of circular-shaped features of approximately 5 – 10 km diameter, given the 5 – 10 km diameter templates. By combining these results with other regional digital information, we hope to reduce the large number of potential impact structures.

This study represents a first screening analysis for potential impact structures in Norway. In addition to analyses of digital elevation data, future programs will explore other types of available regional digital information. This could be satellite data (e.g. radar) and geophysical data (e.g. gravity, magnetic). Geophysical characteristics have been studied for many impact structures and a negative, often circular, gravity anomaly which changes density after impact, is common (Pilkington & Grieve 1992). Magnetic anomalies display large variations across impact craters, but a magnetic low is often a dominant effect (Pilkington & Grieve 1992). The nature of the geophysical signatures implies that using different digital terrain and image analysis techniques (e.g. geomorphometry, Hough transforms), and considering just the circumform shape and not a depression, might be rewarding. Different data may be analysed separately or in combination in order to reduce the number of potential impact structure candidates, and hopefully to find new promising ones.

*Acknowledgments:* This study was funded by the University of Oslo (Department of Geosciences, the Faculty of Mathematics and Natural Sciences, Central Administration) and the Research Council of Norway (NFR#170617/v30). The analyses were carried out at the Laboratory of Remote Sensing and GIS at the Department of Geosciences, Division for Physical Geograpy, University of Oslo. Based on an earlier template version (deeper) and a manual inspection of the resulting sites, 1200 structures were presented on a website ([www.geo.uio.no/groper](http://www.geo.uio.no/groper)) (only in Norwegian). A national school project was launched in cooperation with The Research Council of Norway, where interested classes or students could visit and do the first simple observations of the structures (NFR#171890). This public involvement may have triggered increased public interest in science. In this connection we thank Marianne Løken, Thomas Keilman and Kate Alice Furøy (The Nysgierrigper Science Knowledge Project, Research Council of Norway) for their inspiring support. The review comments by H. Henkel and S.C. Werner significantly improved the manuscript. Thanks to guest editor Odleiv Olesen for editorial handling of the manuscript. We want to thank all individuals and institutions.

## References

- Abels, A. 2006: <<http://www.geophysics.helsinki.fi/tutkimus/impacts/maps.html>> (Accessed: 1 Feb 2006)
- Abels, A., Plado, J., Pesonen, L.J. & Lehtinen, M. 2002: The impact cratering record of Fennoscandia - a close look at the database. In Plado, J. & Pesonen, L.J. (eds.): *Impacts in Precambrian Shields*, 1-58. Springer, Berlin Heidelberg.
- Araujo, A.A., Hadad, R. & Martins Jr, P. 2001: *Identification of pattern in satellite imagery - circular forms*. Nonlinear Image Processing and Pattern analysis, XII, Proceedings of SPIE, 25-34.
- Bruzzone, L., Lizzi, L., Marchetti, P.G., Earl, J. & Milnes, M. 2004: *Recognition and detection of impact craters from EO products*. Proceedings of ESA-EUSC 2004 - Theory and Applications of Knowledge-Driven Image Information Mining with Focus on Earth Observation, Madrid
- Burrough, P.A. & McDonnell, R.A. 1998: *Principles of Geographical Information Systems*. Oxford University Press, Oxford, 333 pp.
- Chicarro, A., Zender, J., Lichtenegger, J., Abels, A., Barbieri, M. & Paoiloni, S. 2003: *ERS Synthetic Aperture Radar Imaging of Impact Craters*. ESA Publications Division, Noordwijk, 69 pp.
- DeMers, M.N. 2002: *GIS modeling in raster*. John Wiley & Sons, New York, 203 pp.
- Di Stadio, F., Costantini, M. & Di Martino, M. 2002. Craters - executive summary: Survey of algorithms for automatic recognition of impact craters. *Telespazio-EO Doc.No. 190.193-SPA-ES-001 - Issue 1.0*. Rome, Italy, ESA contract report, [http://www.esa.int/gsp/completed/ExecSumAll01\\_A19.pdf](http://www.esa.int/gsp/completed/ExecSumAll01_A19.pdf), 28 pp.
- Earl, J., Chicarro, A., Koeberl, C., Marchetti, P.G. & Milnes, M. 2005: *Automatic recognition of crater-like structures in terrestrial and planetary images*. Lunar and Planetary Science XXXVI, Lunar and Planetary Institute, Houston, USA, abstract no. 1319.
- Earth Impact Database. 2006: <<http://www.unb.ca/passc/ImpactDatabase/>> (Accessed: 1 Mar 2006)
- Efford, N. 2000: *Digital Image Processing, a practical introduction using Java*. Addison-Wesley, Harlow, 340 pp.
- Gjessing, J. 1967: Norway's paleic surface. *Norsk Geografisk Tidsskrift* 21, 69-132.
- Gonzalez, R.C. & Woods, R.E. 1993: *Digital Image Processing*, 1st Edition. Addison-Wesley, Reading, Massachusetts, 703 pp.
- Grieve, R.A.F. 1990: Impact cratering on the Earth. *Scientific American* 262, 44-51.
- Grieve, R.A.F. & Pesonen, L.J. 1992: The terrestrial impact cratering record. *Tectonophysics* 216, 1-30.
- Heipke, C. 1997: Automation of interior, relative, and absolute orientation. *ISPRS Journal of Photogrammetry & Remote Sensing* 52, 1-19.
- Hough, P.V.C. 1962: *Methods and Means for Recognizing Complex Patterns*. U.S. Patent No. 3069654 pp.
- Kim, J.R., Muller, J.-P. & Morley, J.G. 2004: *Quantitative Assessment of automated crater detection on Mars*. XXth ISPRS Congress, Istanbul, Turkey, pp. 816-821.
- Kleman, J. & Borgström, I. 1994: Glacial landforms indicative of a partly frozen bed. *Journal of Glaciology* 40, 255-264.
- Lidmar-Bergström, K., Ollier, C.D. & Sulebak, J.R. 2000: Landforms and uplift history of southern Norway. *Global and Planetary Change* 24, 211-231.
- Lowman, P. 1997: Extraterrestrial impact craters. *Oklahoma Geological Survey Circular* 100, 55-81.
- Magee, M., Chapman, C.R., Dellenback, S.W., Enke, B., Merline, W.J. & Rigney, M.P. 2003: *Automated identification of Martian craters using image processing*. Lunar and Planetary Science XXXIV, Lunar and Planetary Institute, Houston, USA, abstract no. 1756.
- Matsumoto, N., Asada, N. & Demura, H. 2005: *Automatic crater recognition on digital terrain model*. Lunar and Planetary Science XXXVI, Lunar and Planetary Institute, Houston, USA, abstract no. 1995.
- Melosh, H.J. 1989: *Impact cratering, A Geologic Process*. Oxford University Press, New York, 240 pp.
- Montanari, A. & Koeberl, C. 2000: *Impact stratigraphy; the Italian record*. Springer-Verlag, Berlin-Heidelberg-New York, 364 pp.
- Niblack, W. 1986: *An Introduction to Digital Image Processing*. Prentice Hall, Englewood Cliffs, 115-116 pp.
- Peulvast, J.-P. 1985: Post-orogenic morphotectonic evolution of the Scandinavian Caledonides during the Mesozoic and Cenozoic. In Gee, D.G. & Sturt, B.A. (eds.): *The Caledonian Orogen - Scandinavia and Related Areas*, 979-995. Wiley, Chichester.
- Pike, R.J. 1977: Size-dependence in the shape of fresh impact craters on the moon. In Roddy, D.J., Pepin, R.O. & Merrill, R.B. (eds.): *Impact and Explosion Cratering*, 489-509. Pergamon Press, New York.
- Pilkington, M. & Grieve, R.A.F. 1992: The geophysical signature of terrestrial impact craters. *Reviews of Geophysics* 30, 161-181.
- Portugal, R.S., de Souza Filho, C.R. & Bland, P.A. 2004: *Automatic crater detection using dem and circular coherency analysis - a case study on south american craters*. 67th Annual Meteoritical Society Meeting, Rio de Janeiro, Brazil, abstract no. 5096.
- Schenk, T. 1999: *Digital photogrammetry*. TerraScience, Laurelville, Ohio, 428 pp.
- Skjeseth, S. 1979: *Innføring i Norges geologi*. Landbruksforlaget Oslo, 37 pp.
- Sollid, J.L. & Sørbel, L. 1994: Distribution of glacial landforms in southern Norway in relation to the thermal regime of the last continental ice-sheet. *Geografiska Annaler* 76, 25-35.
- Strøm, K. 1948: The geomorphology of Norway. *Geographical Journal* CXII, 19-27.
- Turtle, E.P., Pierazzo, E., Collins, G.S., Osinski, G.R., Melosh, H.J., Morgan, J.V. & Reimold, W.U. 2005: Impact structures: What does crater diameter mean? In Kenkmann, T., Hörz, F. & Deutch, A. (eds.): *Large meteorite impacts III: Geological Society of America Special Paper* 384, 1-24.